Sixth International Symposium on Marine Propulsors
smp'19, Rome, Italy, May 2019

The Numerical Analysis of Influence of the Hull Heave Motion on the Propeller Exciting Force Characteristics

Liang Li [1], Bin Zhou[1], Dengcheng Liu[1] , Chaosheng Zheng[1]

[1] China Ship Scientific Research Center (CSSRC) national key laboratory on ship vibration & noise, Jiangsu Key laboratory of Green Ship technology, Wuxi, Jiangsu, China

ABSTRACT

In order to analyze the influence of hull heave motion on the propeller exciting force characteristics, the calculation was performed for the KCS ship and KP505 propeller system in the condition without heave motion and with heave motion by employing Reynolds-Averaged Navier Stokes (RANS) method and adopting the overset grid. The results show that the space non-uniformity of nominal wake in disk plane with heave motion is comparable to the case without heave motion. However, the time non-uniformity increase sharply and it can be predicted that this may leads to worse exciting force performance. Then, through the comparative analysis of hydrodynamic performance and the exciting force performance, it's found that both the hull and propeller hydrodynamic performance deteriorate dramatically due to the heave motion. What's more, the spectrum peaks of exciting force are richer comparing with the condition without heave motion after the fast Fourier transform. And the peak at the heave motion frequency is dominate in all the peak values and shows linear dependence on motion amplitude and the larger the amplitude is, the higher the heave frequency peak will be.

Keywords

Heave motion, Propeller exciting force, wake non-uniformity, Numerical analysis, Hull-propeller-rudder system

1 INTRODUCTION

The high speed and large-scale ships inevitably navigate in the rough sea condition. With the influence of the wind, wave and wake, a significant hull motion in six degrees of freedom will be caused. As the propeller is fixed on the stern, the hull motion, especially for heave and pitch motion, greatly affect the propeller's hydrodynamic performance. The propeller works in the wake changing periodically. As a result, the propeller efficiency will decrease and at the same time the exciting force of propeller increase sharply, which is unfavorable for ship's vibration and noise performance. Therefore, it's important to analysis the influence of the hull motion due to the wind and waves on the propeller exciting force characteristics.

Researchers have done quite a lot of work about the ship and propeller's hydrodynamic performance in the wind waves or motion condition. **Xin Yu (2008)** analyzed the hydrodynamic performance of propeller in wave by simplifying the problem into two aspects. One is the change of propeller axis submergence depth due to the wave. Another is interference of wave diffraction. **Kinnas and Tian (2012)** combined vortex lattice method (VLM) with boundary element method (BEM) to predict the unsteady hydrodynamic analysis of propeller under surge and heave motion. However the effects of turbulence and vortical separated flows are difficult to be handled by this method, resulting in some difference between the calculated results and the RANS simulation results. **Tezdogan and Incecik (2016)** carried out a numerical study of ship motions in shallow water for a full-scale large tanker model and obtained its heave and pitch response to head waves at various depths. The numerical results were found to be in good agreement with the experimental data.

Lianzhou and Chunyu (2017) conducted a numerical simulation on a propeller impacted by heave motion in cavitating flow using the RANS method. The results show that the heave motion would aggravate the unsteady characteristics of thrust and torque coefficient and lead to a non-uniform distribution of propeller sheet cavitation. From the literature survey, it was found that many of previous studies its research objects was the simple foil or single ship and single propeller. The coupled effect between the propeller and ship was not taken into consideration. Moreover, the attention was not paid much to the propeller exciting force performance.

In the present study, the KCS "hull-propeller-rudder" system was employed to analysis the influence of the hull

heave motion on propeller exciting force characteristics employing the RANS method. The heave motion was simplified as a periodic motion based on a sinusoidal function and was achieved by overset grid method. The change rule and characteristics of hull resistance, wake field and propeller exciting force was successfully obtained and the results can provide important reference for the prediction of full-scale ship's hydrodynamic performance in motion condition.

2 MATHEMATIC BASE

2.1 Governing Equations

Fluid flow is governed by physical conservation laws. Basic conservation laws include law of conservation of mass, law of conservation of momentum and law of conservation of energy **(David C. Wilcox, 1994)**. As the medium in our calculation, water, is an incompressible fluid whose heat exchange is little enough to ignore, only the mass conservation equation and the momentum conservation equation are solved.

$$\frac{\partial \rho}{\partial t}+\frac{\partial(\rho u_i)}{\partial x_i}=0 \tag{1}$$

$$\frac{\partial(\rho u_i)}{\partial t}+\frac{\partial}{\partial x_j}(\rho u_i u_j)=-\frac{\partial p}{\partial x_j}+\frac{\partial}{\partial x_j}(\mu\frac{\partial u_i}{\partial x_j}-\rho\overline{u_i' u_j'})+S_j \tag{2}$$

Here, u_i and u_j is the averaged Cartesian components of the velocity vector (i , j=1,2,3). p is the mean pressure. ρ is the fluid density and μ is the dynamic viscosity. $\rho\overline{u_i' u_j'}$ is the Reynolds stresses. S_j is the generalized source term of the momentum equation.

2.2 Turbulence Model and Free Surface Model

The governing equations is solved using segregated method based on pressure-velocity, in which the second upwind scheme is used for the discretization of convective term and the second central differencing scheme is used for the discretization of dissipation term. In order to simulate the flow separation and strong adverse pressure gradients well, the SST (Shear Stress Transport) $k-\omega$ turbulence model is adopted (**Menter, 1994**). This model effectively integrates the merits of both $k-\varepsilon$ and $k-\omega$ models and is the one of the most advanced two-equation turbulence model currently, which has a good advantages in calculating the viscous flow around bodies. But a certain range of Y plus value is needed for this model, in general, the Y plus being set to 30~200 is proper. The free surface is modeled by Volume of Fluid (VOF) method(**Karim and Prasad, 2014**), whose essential is to determine the free surface by investigating the fluid-grid volume fraction function in the grid cells and trace the variation of the fluid rather than the particle movement on the free surface. As long as the value of the function on each grid of the flow field is known, the movement interface can be traced.

2.3 Overset Grid

The hull heave motion is simulated by overset grid method (**Carrica and Wilson, 2007**). Compared to the general dynamic mesh, the overset grid is more adaptable and efficient in dealing with the large-amplitude motion. The overset grid method divides the computational domain into a number of subdomains whose grids are generated independently. Information transmission is implemented through grid nesting and overlap in these subdomains. In the boundary flow fields of the overset grids, information is coupled through interpolation. The overset grid generation involves two main steps: a "hole-cutting" operation on the grids of the background domain to shield the area inside the hole, mark those grids within the hole, and abandon them in the subsequent CFD computation; and a "point-searching" operation to interpolate information transmitted at the hole boundaries for the subsequent numerical calculation. The schematic of overset grid is shown in **Figure 1**.

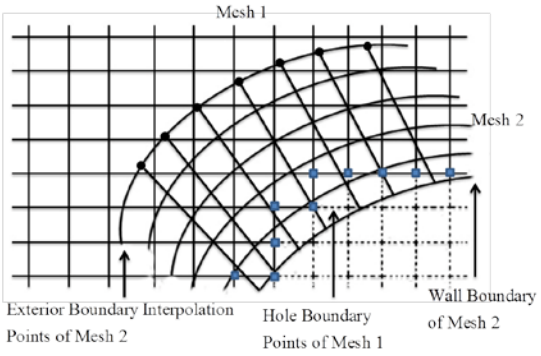

Figure 1 Schematic of overset grid

3 CALCULATION MODELING

3.1 Calculation object

The standard model KCS container ship with the scale factor of 31.6 is used as the study objects as **Figure 2** shows, whose principle parameters is listed in **Table 1**. The notable bulbous bow and stern extension will result in complex wake and wave，which can provide good wake environment to study the propeller exciting force characteristics. The propeller that goes with the ship is a KP505 propeller. The propeller principle parameters is given in **Table 2**.

Figure 2 KCS ship and KP505 propeller geometry model

Table 1 Principle parameters of KCS model

L_{pp}（m）	7.2786
Draught（m）	0.3418
Wetted surface（m^2）	9.438
Reynolds No.	1.4×10^7
Froude No.	0.26

Table 2 Principle parameters of KP505 propeller model

Diameter（m）	0.250	Area ratio	0.70
No. of blades	5	P/D（0.7R）	1.00
Hub ratio	0.167	Skew angle（°）	12.66

3.2 Computational Domain and Boundary Condition

In order to simulate the hull heave motion, the computational domain is divided into background domain and overset grid domain as **Figure 3** shows. The background domain is set as a cuboid water basin referring the towing tank. The inlet is $2L_{pp}$ from the bow to ensure the inflow is uniform. The domain side and bottom from the hull surface are both $2L_{pp}$ to avoid the hull flow field affected by the basin wall. And taking the fully development of hull wake into account, the outlet from the stern is $3L_{pp}$. The inlet is set as a velocity inlet. The outlet is set as a pressure outlet. The domain top plane is set as a symmetry and the other boundaries are set as a wall. The overset grid domain is nested in the background domain, which includes the hull-propeller-rudder model and can realize the simulation of hull heave motion.

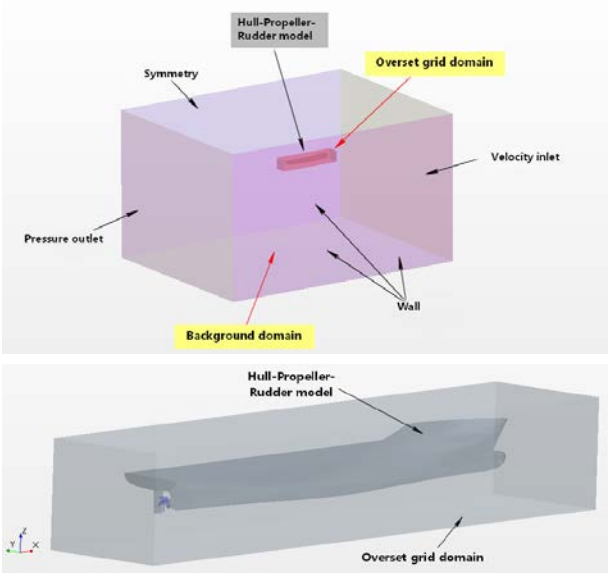

Figure 3 Computational domain and boundary condition

3.3 Grid Division

In our calculation, the trimmer mesh is used. It can capture the boundary layer flow effectively as well as control the total grid number of calculation. The grid division detail is shown in **Figure 4**. When perform the grid division, the grid size of background domain around the overset area at best keep the same with the grid size at the overset grid boundary. What's more, the motion range of overset grid should be limited within the overset area. Regarding to the hull surface mesh, more grids should be given to the bow and stern of the hull where flow field varies dramatically. To capture the free surface better, the grids near the free surface and within the range of Kelvin waves are properly refined. The first layer of grids is 0.8~1 mm, corresponding to which the Y plus is about 60. Based on the previous calculating experience, the total grids number is set as 4.5 million to save the computational time, but a satisfied calculation accuracy can also be reached.

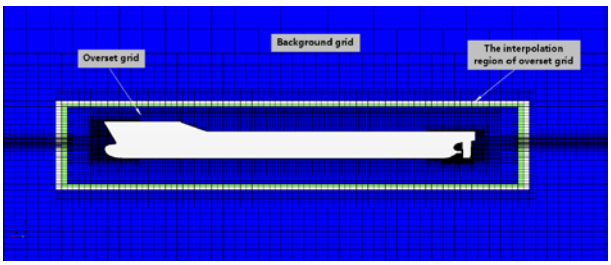

（a）The distribution of overset grid

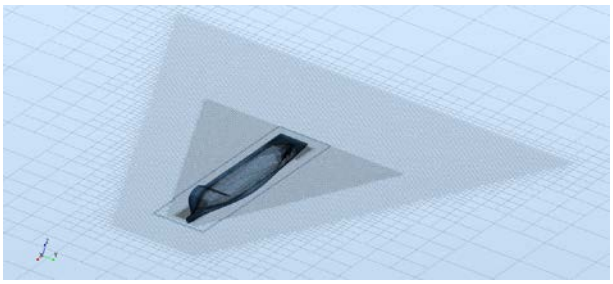

（b）The grids near the free surface

（c）Hull surface grids

Figure 4 Computational grid distribution

3.4 Calculation Conditions and Setting of Motion Model

The calculation is performed by two steps. At the first step, only the hull and rudder model are used to investigate the change rule of propeller inflow in heave motion. Then the propeller is taken into consideration as a whole system to get the exciting force data. In this study, the heave motion is defined independently using sinusoidal function as follows:

$$y(t) = A_p \sin(\omega(t - \Delta t) \tag{3}$$

Here, y is the moving distance of hull in vertical direction, corresponding with the moving distance at z direction in the present calculating coordinate system and upward is positive. A_p is the amplitude of the heave motion and is selected as $0.25T_m$ and $0.125\ T_m$ in the calculation by taking the amplitude of the forced oscillation model test as reference. Where T_m represents the draft depth in the static water. ω is the frequency of heave motion and is dependent on the heave period T_e . T_e is selected as 2 second in this work. Δt is the delay time to ensure the numerical stability, being selected as 26 seconds, at which the hull system is without the heave motion. The schematic plan of heave motion rule is shown as **Figure 5**.

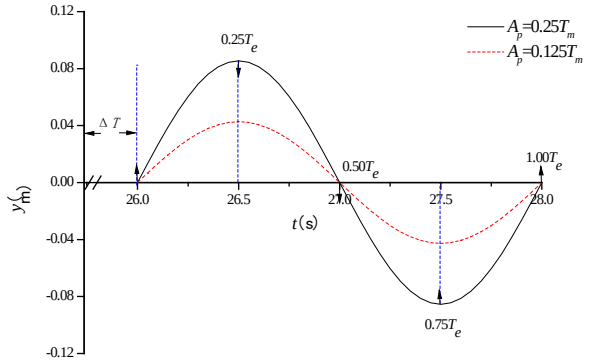

Figure 5 Schematic plan of heave motion rule

The difficulty to simulate the motion of hull-propeller system is how to realize the superimposition of hull heave motion on the propeller rotating motion without hull-propeller model separation showing in the process of simulation. In order to handle this problem, superimposed coordinate system method is applied. So three different coordinate systems are created, including the initial coordinate system, a new local hull coordinate system and a new local propeller coordinate system. The original point of initial coordinate system is located in the crossing point of after-perpendicular and free surface. The original point of initial coordinate system is located in the mass centre of hull. The original point of initial coordinate system is located in the crossing point of propeller axis and propeller disk. The details is shown in **Figure 6**. It can be seen that it's convenient to define the hull heave motion in the local hull coordinate system, so it is with the propeller's rotation motion in the local propeller coordinate system. Then the superimposed motion can be realized by attaching the locale propeller coordinate system to the hull heave motion in the local hull coordinate system.

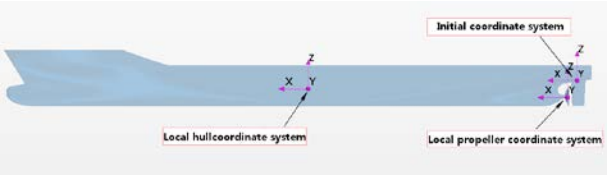

Figure 6 Schematic plan of different coordinate systems

4 RESULTS ANALYSIS

4.1 Validation of Calculation Method

Firstly, the numerical calculation for both the bare hull and hull-propeller-rudder system are performed without heave motion to validate the calculation method with the condition that the flow speed is 2.196m/s, the propeller revolution speed is 9.5 rps and the draft is 0.3418m. The time step is set as the time in which the propeller rotates for 4 degrees.

The **Table 3** shows the hydrodynamic calculation results. In general, it shows good agreements with the experimental data (**Larsson and Stern, 2013**). The error of propeller thrust is the biggest, but it is still under the 5% that can be accepted. The possible reasons for this are the neglecting of the hull posture change during the calculation and the presence of the rudder in this work.

Figure 7 shows the comparison between EFD and CFD for wave contour. It can be seen that the values and position of the peaks and troughs are consistent between EFD and CFD. The previous problems that wave on the hull both side dissipate too quickly and the details for broken wave at stern are not caught well are improved effectively by logical grid division strategy.

Figure 8 shows the comparison between EFD and CFD for velocity contour. The calculated values also show good agreement with EFD's. But the shrinkage of velocity contour of EFD towards the midship section is more serious that means the boundary layer is thinner in the experimental condition. The use of boundary layer trip in test may cause this phenomenon happen. Overall, the calculation method used in this work is accurate and satisfactory.

Table 3 Hydrodynamic calculation results of hull-propeller-rudder system

	Resistance F_s /N	Thrust T/N	Moment M/N.m
CFD (with rudder)	90.5	57.22	2.62
EFD (without rudder)	90.0	59.9	2.53
Error	+0.56%	-4.47%	+1.58%

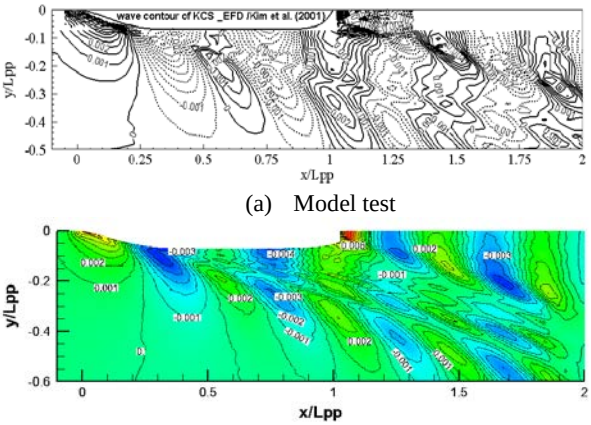

(a) Model test

(b) CFD calculation

Figure 7 Comparison for wave contour

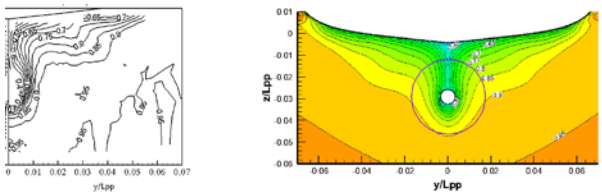

(a) Model test (b) CFD calculation

Figure 8 Comparison for velocity contour ($x / L_{pp} = 0.9825$)

4.2 Wake analysis

The propeller exciting force performance is strongly associated with the wake non-uniformity. When the ship sail normally without a large amplitude motion, the wake temporal non-uniformity induced by flow turbulence characteristics is slight. The spatial wake temporal non-uniformity is the dominant factor affecting the propeller

exciting force. But when the ship sail in rough sea with a significant heave or pitch motion, the wake temporal non-uniformity caused by motion period is non-negligible. The priority is given to axial wake in three directional wake. To analysis the non-uniformity of axial wake, the axial velocity is non-dimensionalized by the inlet velocity (2.196 m/s). The spatial non-uniformity is defined as:

$$\overline{u}_x'(r)=\frac{1}{2\pi}\int_0^{2\pi}u_x'(r,\theta)d\theta \tag{4}$$

$$\Delta' u_x'(r)=\frac{(u_x'(r))_{\max}-(u_x'(r))_{\min}}{\overline{u}_x'(r)} \tag{5}$$

Here, u_x' is the dimensionless axial velocity. $\overline{u}_x'(r)$ is the circumferential average of dimensionless axial velocity in a specific radius. $(u_x'(r))_{\max}$ is the peak value in a specific radius and $(u_x'(r))_{\min}$ is the valley value. $\Delta' u_x'(r)$ is the spatial non-uniformity. The bigger the spatial non-uniformity is, the worse the propeller exciting force performance will be.The temporal non-uniformity is defined as:

$$\overline{u_x'}(t)=\frac{1}{S}\iint_s u_x'(r,\theta,t)rd\theta dr \tag{6}$$

$$\overline{u_x'}=\frac{1}{T_e}\int_0^{T_e}\overline{u_x'}(t)dt \tag{7}$$

$$\Delta' u_x'=\frac{(u_x'(t))_{\max}-(u_x'(t))_{\min}}{\overline{u_x'}} \tag{8}$$

Here, $\overline{u_x'}(t)$ is the disk surface average of dimensionless axial velocity in a specific time. $\overline{u_x'}$ is the time average of disk dimensionless axial velocity. $\Delta' u_x'$ is the temporal non-uniformity in a motion period which is defined similarly with the spatial non-uniformity.

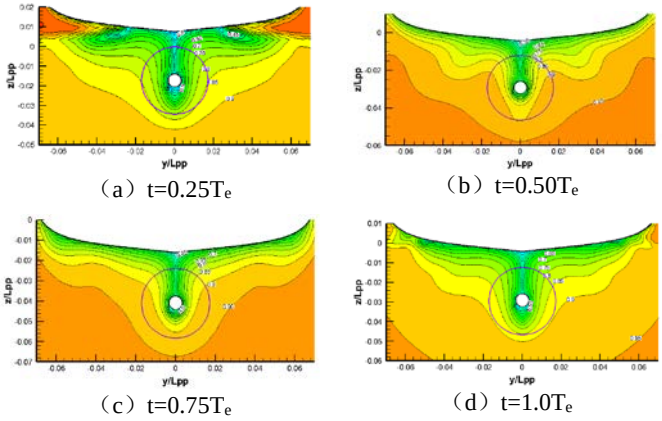

（a）t=0.25Te　（b）t=0.50Te

（c）t=0.75Te　（d）t=1.0Te

Figure 9 Distribution of the nominal wake fields at different time ($x/L_{pp}=0.9825$)

Figure 9 shows the distribution of the nominal wake fields at different time. Since the flow field at 0.7R radius has a dominant influence for propeller hydrodynamic performance, the spatial non-uniformity of nominal wake is analyzed by taking the axial velocity at 0.7R radius for as a represent. **Figure 10** shows the circumferential distribution of axial velocity at different time. The analysis results of the spatial non-uniformity are listed at **Table 4**. In general, the hull heave motion doesn't make the spatial non-uniformity become worse. Reversely, there is some improvement at the time that the hull draft is deeper for example when t is $0.75T_e$.

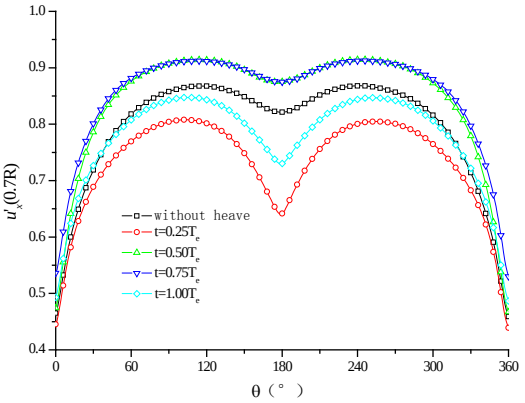

Figure 10 Circumferential distribution of axial velocity at different time for 0.7R radius ($A_p=0.25T_m$)

Table 4 Spatial non-uniformity of axial velocity at different time for 0.7R radius ($A_p=0.25T_m$)

	Without heave	$0.25T_e$	$0.50T_e$	$0.75T_e$	$1.0T_e$
Average value	0.796	0.731	0.846	0.855	0.777
Peak value	0.868	0.808	0.915	0.913	0.847
Valley value	0.459	0.439	0.467	0.530	0.486
Spatial non-uniformity (%)	51.37	50.45	52.85	44.76	46.44

Figure 11 shows the average axial velocity curve at disk plane in a motion period. From the analysis results listed in **Table 5**, we can know that compared with the condition without heave motion, the temporal non-uniformity increase sharply from 0.11% to 9.28% and 17.78%. It also shows that the temporal non-uniformity has a significant positive relationship with the heave motion amplitude.

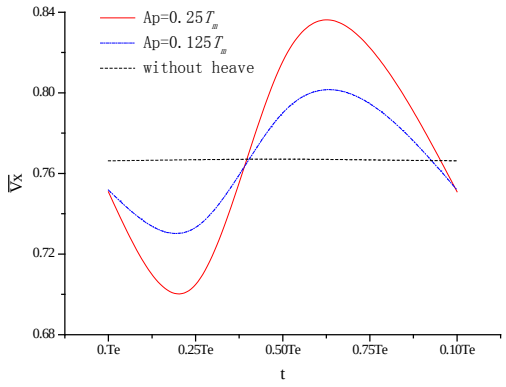

Figure 11 Average axial velocity curve at disk plane in a motion period

Table 5 Temporal non-uniformity of axial velocity for different heave amplitude

	Without heave	$A_p=0.25T_m$	$A_p=0.125T_m$
Average value	0.7666	0.7661	0.7677
Peak value	0.7671	0.8361	0.8014
Valley value	0.7663	0.6999	0.7301
Temporal non-uniformity (%)	0.11	17.78	9.28

4.3 Hydrodynamic Performance Analysis

Ship resistance will be affected by heave motion because of the changes of wetted surface area and wave patterns around the ship. **Table 6** lists the calculation results of resistance. The resistance increase percent is 54.23% when the heave amplitude was $0.25T_m$ and the resistance increase percent is 18.80% when the heave amplitude was $0.125T_m$. It shows that the resistance increase dramatically in the condition of heave motion and the bigger the motion amplitude is, the more significant the resistance increase will be. **Figure 12** has given the wave contour on the hull surface in a motion period.

Table 6 Time average resistance in heave motion

	Without heave	$A_p = 0.25T_m$	$A_p = 0.125T_m$
Time average resistance（N）	90.50	139.58	107.52
Resistance increase percent（%）	—	54.23	18.80

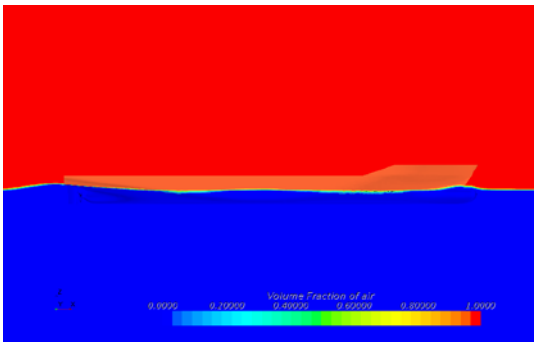

（a）t=0.25Te

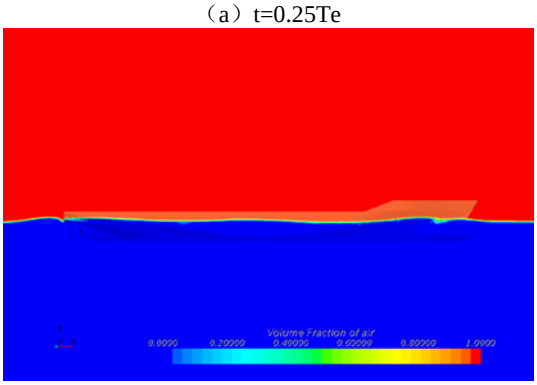

（b）t=0.50Te

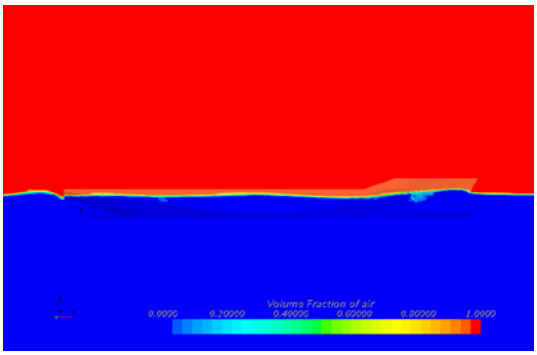

（c）t=0.75Te

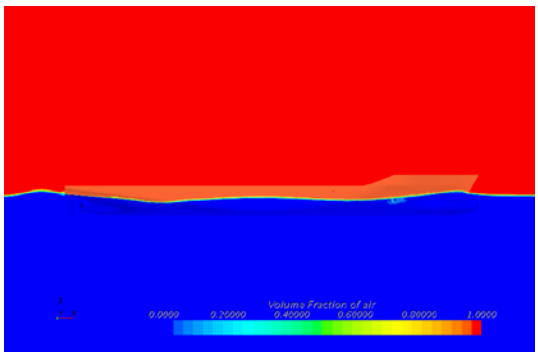

（d）t=1.0Te

Figure 12 Wave contour on the hull surface in a motion period

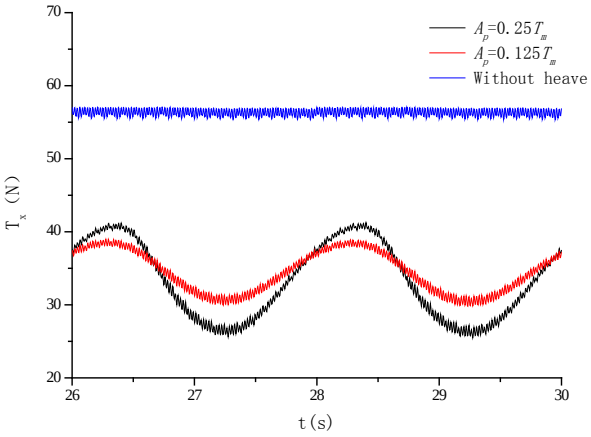

Figure 13 Time domain curves of thrust with heave motion

Figure 13 shows the Thrust change curves in time domain. There are two points that need to be paid attention to in the heave motion. The first point is the large drop of thrust that will affect ship speed strongly. The second point is the large fluctuating amplitude of thrust that will be bad to ship vibration and noise performance.

4.4 Propeller Exciting Force Analysis

The propeller exciting force in frequency domain was obtained after performing the FFT transformation for time domain signal. **Figure 14** shows frequency domain curves of the propeller exciting force without heave motion. Here, the F_x is the thrust, F_y is the horizontal force, F_z is the vertical force. It can be concluded that the propeller thrust and side force have the same fluctuation frequency. Peaks appear at the axial frequency (9.5Hz), blade frequency (47.5 Hz), double blade frequency (95.0 Hz) and triple blade frequency (142.5 Hz), with the peak being the largest at the BPF and quickly attenuating afterwards. After 3BPF, these forces can be ignored. The peaks between the thrust and side force don't show obvious differences and that is because the propeller works in the non-uniform wake, the blades can't balance the force in *Y*, *Z* direction well. Although the time average of side force is not very large, the fluctuating amplitude is comparable with the thrust.

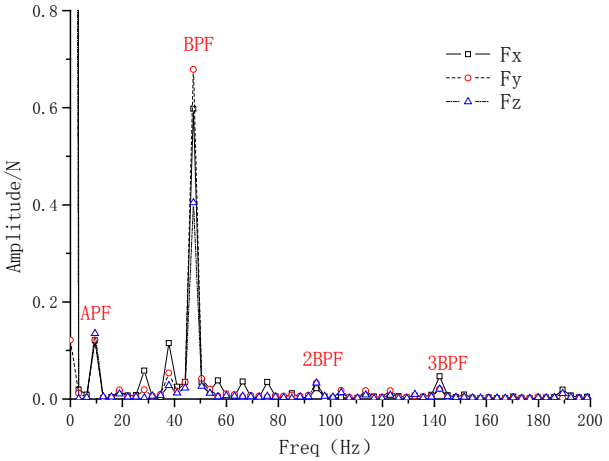

Figure 14 Frequency domain curves of propeller exciting force without heave motion

Frequency domain curves of propeller exciting force with heave motion is shown from **Figure 15** to **Figure 17**. Compared with results without heave motion, the following rules can be concluded.

(1) Spectrum peaks are richer in heave motion condition. Except for the original blade frequency and axis frequency, the peaks also show in heave frequency (0.5Hz), double heave frequency (1.0Hz) and triple heave frequency (1.5Hz) to some degree.

(2) The peaks at blade frequency which is induced mainly by spatial non-uniformity at disk plane, is comparable with its value in the condition without heave motion. This rule correspond with the wake analysis results that heave motion doesn't has much influence on spatial non-uniformity at disk plane.

(3) The peaks at heave frequency which is induced mainly by temporal non-uniformity at disk plane, is much bigger than its at blade frequency and it has become the main fluctuating quantity except for horizontal force. It means that temporal non-uniformity, comparing with spatial non-uniformity, is the main factor affecting propeller exciting force performance in heave motion condition. And the side force peak at motion frequency is related with hull motion direction.

(4) The peak at heave frequency shows linear dependence on motion amplitude and the larger the amplitude is, the higher the heave frequency peak will be. However, the peak at blade frequency is almost the same for different motion amplitude.

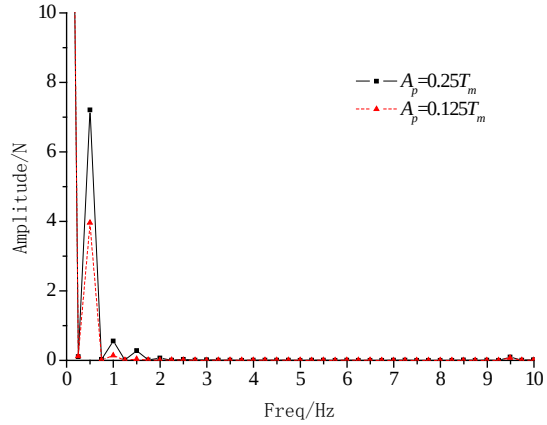

(a) 0~10 Hz

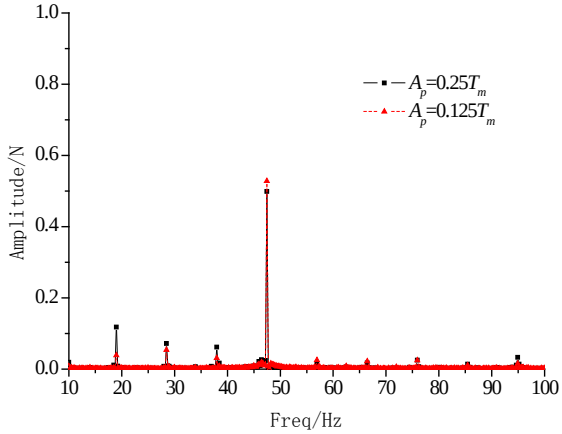

(b) 10~100 Hz

Figure 15 Frequency domain curves of thrust with heave motion

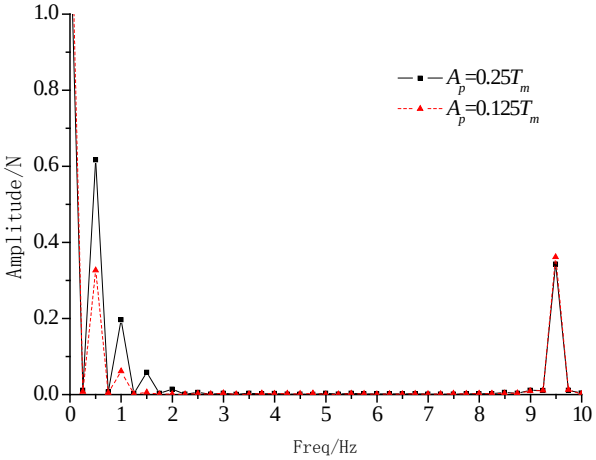

(a) 0~10 Hz

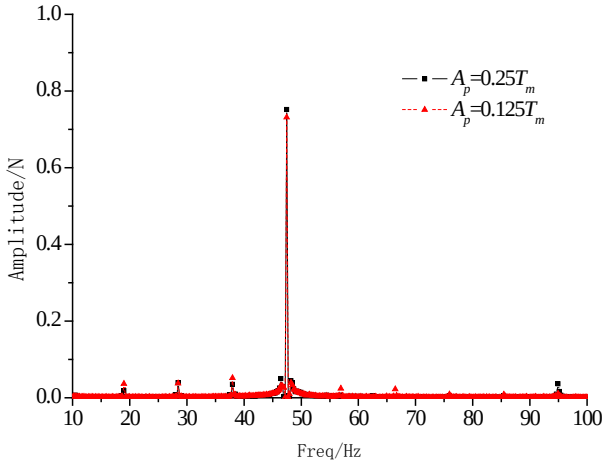

(b) 10~100 Hz

Figure 16 Frequency domain curves of horizontal force with heave motion

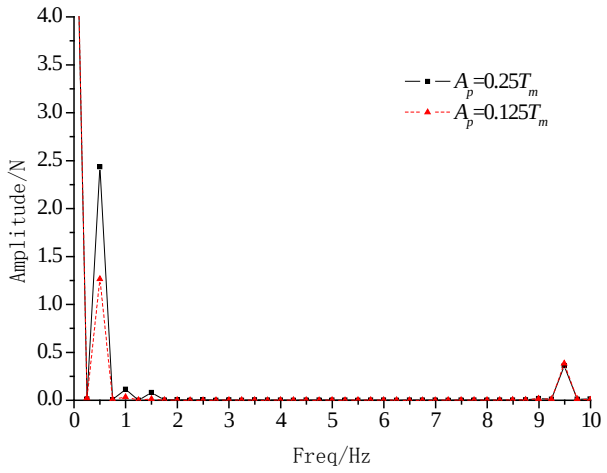

(a) 0~10 Hz

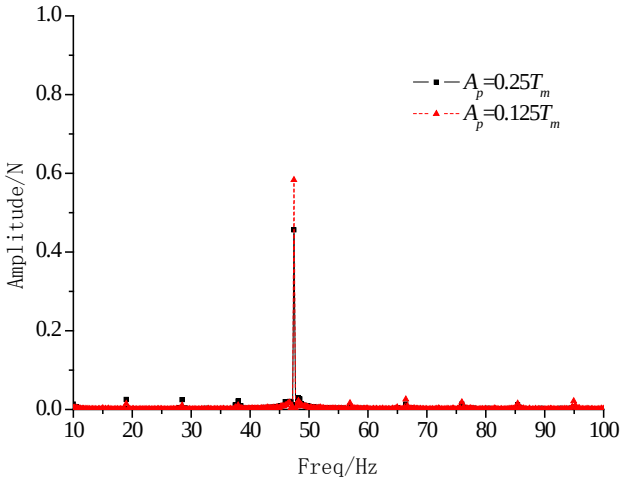

(b) 10~100 Hz

Figure 17 Frequency domain curves of vertical force with heave motion

5 CONCLUSIONS

The numerical simulation has been conducted on the KCS ship and KP505 propeller system with heave motion by employing RANS method and overset grid method. Through the comparative analysis of hydrodynamic performance and the exciting force performance, the conclusions are obtained as follow. From the analysis of wake field, we can know that the hull heave motion leads little changes to the disk wake spatial non-uniformity. However, the temporal non-uniformity in heave motion increase dramatically compared with case without heave motion. Furthermore, the increase of resistance and the drop of thrust induced by heave motion are also significant which may lead to an obvious speed lose. On the other hand, the thrust in heave motion fluctuate more strongly than the case without heave motion. Through a further analysis for frequency domain curves of propeller exciting force, we can know that spectrum peaks are richer in heave motion condition. Some peaks related to the heave frequency and its integral multiples are shown. The peak at heave frequency (0.5Hz) is much bigger than the peak at blade frequency (47.5Hz) and it has become the main fluctuating quantity except for horizontal force. What's more, the peak at heave frequency shows linear dependence on motion amplitude and the larger the amplitude is, the higher the heave frequency peak will be.

REFERENCES

Xin Yu. (2008). 'Research on hydrodynamic performance of propeller in heaving condition'. MS thesis, Harbin Engineering University, China.

Kinnas S. A. & Tian Y. (2012). 'Numerical modeling of a marine propeller undergoing surge and heave motion'. International Journal of Rotating Machinery, Austin, USA.

Tezdogan T. & Incecik A. (2016). 'Full-scale unsteady RANS simulations of vertical ship motions in shallow water'. Ocean Engineering, 123, pp.131-145.

Lianzhou W. & Chunyu G. (2017). 'Numerical analysis of a propeller during heave motion in cavitating flow'. Applied Ocean Research. 66, pp.131-145.

David C.Wilcox (ed.) (1994). 'Turbulence Modeling for CFD'. DOW Industries, Inc. La Can(~)ada, California, USA.

Menter F.R. (1994). 'Two-equation eddy-viscosity turbulence models for engineering applications'. AIAA J. 32 (8), pp.1598–1605.

Karim, M.M. & Prasad B.R. (2014). 'Numerical simulation of free surface water wave for the flow around NACA 0015 hydrofoil using the volume of fluid (VOF) method'. Ocean Engineering, 78, pp.89-94.

Carrica P.M. & Wilson R.V. (2007). 'Ship motions using single-phase level set with dynamic overset grids'. Comput. Fluids. 36 (9), pp.1415–1433.

Larsson L. & Stern F. (2013). 'CFD in Ship Hydrodynamics- Results of the Gothenburg 2010Workshop'. MARINE 2011, IV International Conference on Computational Methods in Marine Engineering. Springer, pp.237-259.